Nonreciprocal Polarization Conversion in Asymmetric Magnetooptic Waveguide

Tomohiro Amemiya, *Member, IEEE,* Kenji Abe, Takuo Tanemura, *Member, IEEE*, Tetsuya Mizumoto, *Member, IEEE*, and Yoshiaki Nakano, *Member, IEEE*

***Abstract*— A nonreciprocal polarization converter compatible with InP photonic integrated circuits is demonstrated. The device consists of an asymmetric InGaAsP waveguide combined with a ferrimagnetic Ce:YIG layer. It makes use of the direction dependence of the propagation of light in the waveguide. A trial device was made using orientation-dependent etching of InGaAsP and wafer-bonding of YIG to InGaAsP. It showed a nonreciprocal TE–TM conversion efficiency of 38% at 1.55 μm wavelength.**

***Index Terms*— Magnetooptic effect, photonic integrated circuits, polarization converter, waveguide optical isolator.**

I. Introduction

AVOIDING problems caused by undesired reflections of light is a matter of great importance in photonic integrated circuits (PICs) [1], [2]. As a promising unilateral device to counter this problem, this paper demonstrates a waveguide-based nonreciprocal polarization converter (NRPC) that can be monolithically combined with devices on a PIC.

A large-scale PIC is composed of a variety of waveguide-based optical devices integrated on an InP substrate to create the desired optical functions in a single chip. In such integrations, connecting optical devices without the backreflection of light along a reverse direction is indispensable because backreflection badly affects and destabilizes the operation of optoelectronic devices such as lasers and amplifiers. To cope with this problem, much effort has been expended in developing waveguide-based unilateral devices that can be integrated monolithically with other optical devices. Leading examples are the nonreciprocal phase-shift isolator [3], [4] and the nonreciprocal loss isolator [5]–[7]. They both make good use of nonreciprocal phenomena in magnetooptic waveguides. However, they are still in the experimental stage and have several problems. The nonreciprocal phase-shift isolator needs a large device length (>2 mm) and a complicated fabrication process because it uses a Mach–Zehnder interferometer. The nonreciprocal loss isolator has a large intrinsic loss caused by its principles of operation and therefore needs a high-gain optical amplifier to compensate for its insertion loss.

To overcome these problems, we previously proposed a novel unilateral device, i.e., a waveguide-based NRPC and showed its operation with theoretical calculations [8]. This device makes use of the nonreciprocal change of polarization in an asymmetric semiconductor waveguide combined with a magnetic garnet.

To materialize our idea, in this paper, we fabricate an actual device and measure its operation to confirm the nonreciprocal TE–TM conversion we expected. Our device is compatible with InP-based PICs and promising as a unilateral coupler to interconnect optical devices in the PIC.

In the following sections, we first outline the concept of our NRPC, the structure and operation principles are explained in Section II. We then describe the actual device made by us. Our device is composed of an asymmetric InGaAsP waveguide combined with a $CeY_2Fe_5O_{12}$ (Ce:YIG) layer and fabricated using the process technology of orientation-dependent InGaAsP etching and YIG-to-InGaAsP wafer bonding (Sec. III). We then measured the transmission of light in the fabricated device. From the experimental data, we estimated the nonreciprocal TE–TM conversion efficiency to be 38% at 1.55 μm wavelength (Sec. IV).

II. Waveguide-Based NRPC: Principle and Structure

The function of an NRPC is the nonreciprocal TE–TM mode conversion of light, as shown in Fig. 1. Incident light with TE polarization passing through an NRPC in the forward direction maintains its TE mode and goes out through the right end. In contrast, backward propagating TE-mode light from the right end is transformed into a TM mode in the NRPC. Inserting an NRPC at the output port of an optical device can suppress the detrimental effect of backreflected light because most optical devices designed for use in TE polarization are insensitive to TM light. [This is so because most active optical devices use compressive-strained quantum wells to induce the heavy-hole and light-hole band splitting (HH–LH splitting). The HHs and LHs interact with TE- and TM-polarized light, respectively, and the HH band is lower in energy than the LH band because of the HH–LH splitting. Therefore, in devices designed for TE-mode operation, TM reflected light with the same wavelength hardly induces stimulated emission in the device.]

Manuscript received March 31, 2010; revised June 5, 2010; accepted June 22, 2010. Date of current version September 8, 2010.

T. Amemiya is with the Quantum Nanoelectronics Research Center, Tokyo Institute of Technology, Tokyo 152-8552, Japan (e-mail: amemiya.t.ab@m.titech.ac.jp).

K. Abe and T. Mizumoto are with the Department of Electrical and Electronic Engineering, Tokyo Institute of Technology, Tokyo 152-8552, Japan (e-mail: abe.k.aa@m.titech.ac.jp; tmizumot@pe.titech.ac.jp).

T. Tanemura and Y. Nakano are with the Research Center for Advanced Science and Technology, University of Tokyo, Tokyo 153-8904, Japan (e-mail: tanemura@hotaka.t.u-tokyo.ac.jp; nakano@ee.t.u-tokyo.ac.jp).

Color versions of one or more of the figures in this paper are available online at http://ieeexplore.ieee.org.

Digital Object Identifier 10.1109/JQE.2010.2058093

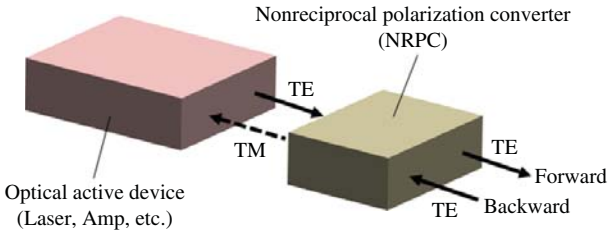

Fig. 1. Function of NRPC.

If necessary, we can make an isolator by attaching a waveguide polarizer or splitter to the NRPC [9], [10].

A. Principle of Waveguide-Based NRPC Device

To make a waveguide NRPC compatible with InP-based PICs, we previously proposed a device shown in Fig. 2(a) (see [8] for details). Our device is a magnetooptic waveguide consisting of an asymmetric InGaAsP waveguide and a ferrimagnetic cerium-substituted yttrium iron garnet (Ce:YIG) layer attached on the top of the waveguide. The InGaAsP waveguide has an asymmetric cross section with a right trapezoid shape, as shown in Fig. 2(b). The YIG layer is magnetized in the x direction, and light travels in the z direction.

Incident TE-polarized light excites two rotated orthogonal modes of polarization [denoted by mode 1 and mode 2 in Fig. 2(b)] in the asymmetric waveguide [11]–[13]. Because of the magnetooptic transverse Kerr effect, the mode birefringence of light traveling in the waveguide differs between forward and backward propagations. As a result, the beat length of light can also be different between forward and backward directions. To make an NRPC, we first set the rotation angle φ of the orthogonal axes to $\pi/4$ so that the incident TE light will excite the two rotated modes equally. We then set the beat length L for backward propagation twice as large as that for forward propagation, that is

$$L = \frac{2\pi}{|\beta_{1f} - \beta_{2f}|} = \frac{\pi}{|\beta_{1b} - \beta_{2b}|} \tag{1}$$

where β_{1f}, β_{2f}, and β_{1b}, β_{2b} are the forward and backward propagation constants of orthogonal modes 1 and 2. These conditions can be satisfied with appropriate values of waveguide parameters w, h, and θ. With these conditions, the two excited modes recombine into a TE mode for the forward propagation and into a TM mode for the backward propagation at distance L from the incidence point. This is illustrated with Fig. 3. Thus, the device with a length L operates as an NRPC.

B. Designing the Structure of the Device

To optimize the structure of the device, we performed electromagnetic calculation to confirm the device operation at 1.55 μm wavelength. We first calculated the distribution of electromagnetic field in the xy plane to determine the optimized cross-sectional structure of the device, with the aid of computer simulation based on the finite-difference method. Then we calculated the propagation pattern of light in the z direction, using the vectorially corrected approach [14], [15]. (See [8] for details of our calculation.)

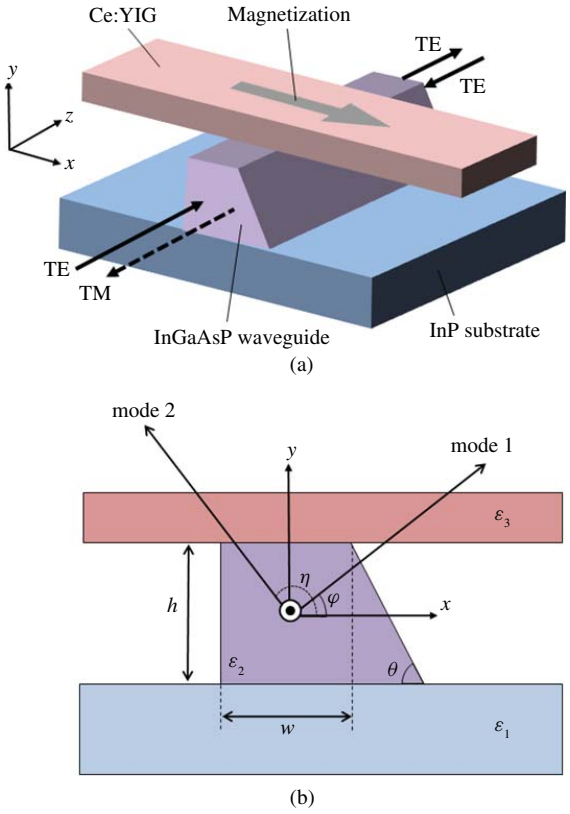

Fig. 2. NRPC consisting of asymmetric InGaAsP waveguide with ferrimagnetic Ce:YIG. (a) 3-D view of NRPC on InP substrate. (b) Cross sectional view.

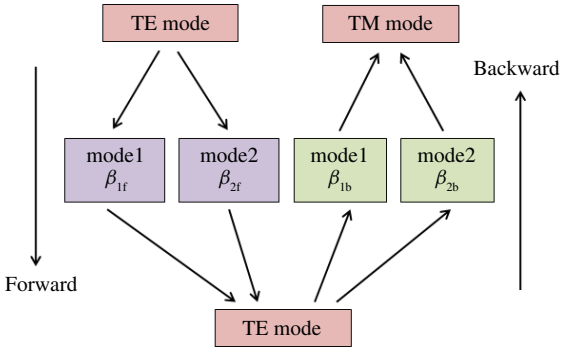

Fig. 3. Principle of nonreciprocal TE–TM conversion. Incident TE mode is resolved into two eigenmodes 1 and 2 with forward propagation constants $\beta_{1f} - \beta_{2f}$ and backward ones $\beta_{1f} - \beta_{2f}$, then recombined into TE mode for forward propagation and into TM mode for backward propagation.

In our calculation, we used the following device parameters. The composition of the InGaAsP waveguide was set to $In_{0.75}Ga_{0.25}As_{0.54}P_{0.46}$ (absorption edge = 1.25 μm). The refractive index is 3.16 for InP, 3.40 for InGaAsP, and 2.2 for Ce:YIG. The Faraday rotation coefficient of Ce:YIG is -4500 deg/cm at 1.55 μm. The base angle θ of the waveguide trapezoid was set to 54° [angle for (111) plane] because, as will be explained in the next section, we made the trapezoid-shaped waveguide by means of orientation-dependent chemical etching of an InGaAsP(100) plane. With the aid of computer simulation, we determined the optimal cross section of the waveguide as $h = 1.1$ μm and $w = 1$ μm.

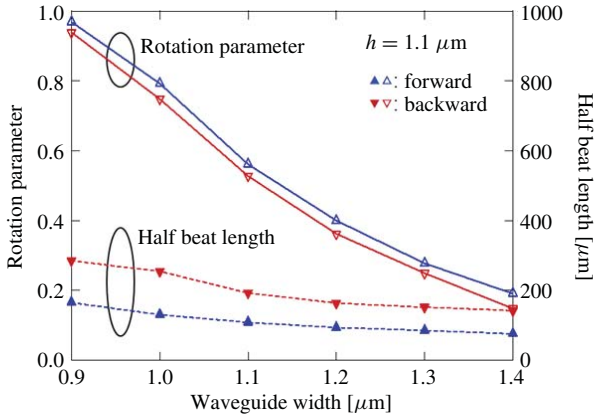

Fig. 4. Half-beat length and rotation parameter as a function of base length w, calculated for altitude $h = 1.1$ μm.

Fig. 4 depicts the calculated values of the half-beat length and the rotation parameter as a function of w for $h = 1.1$ μm. The rotation parameter R gives the angles φ and η [see Fig. 2(b)] of eigenmodes as

$$|\varphi| = \left|tan^{-1}(R)\right|, \quad |\eta| = \left|tan^{-1}\left(-\frac{1}{R}\right)\right|. \tag{2}$$

The efficiency of TE–TM conversion takes the maximum at a distance of half-beat length, and the maximum value increases as R increases. A complete conversion can be obtained for $R = 1$; that is, angle φ should be $\pi/4$. The rotation parameter decreases as w and h increase. This is so because light is mainly distributed in the central part of the waveguide, and therefore an increase in the cross-sectional size of the waveguide decreases the asymmetry that light experiences during its propagation.

The necessary conditions for efficient nonreciprocal conversion are: 1) rotation parameter $R = 1$ to achieve a complete TE–TM conversion, and 2) backward half-beat length twice as large as forward one so as to satisfy (1). With the results of Fig. 4, we determined the optimal cross-sectional structure of the waveguide to be $w = 1.0$ μm and $h = 1.1$ μm. In this simulation, smaller devices ($w < 0.9$ μm) were not taken into account because it is not easy to make such small devices with our existing process technology.

For TE-polarized incident light, we calculated the power distribution of light along the z-axis in the waveguide. Fig. 5 shows the results plotted as a function of propagation distance for forward [Fig. 5(a)] and backward [Fig. 5(b)] propagation. There is no TM component at $z = 0$ because we assumed a TE-polarized input. As light travels in the waveguide, polarization conversion between TE and TM is repeated periodically. The period for backward propagation is twice as large as that for forward propagation, and this causes the nonreciprocal conversion. Forward-propagating TE-mode light returns to TE mode after traveling a distance of 0.27 mm, which corresponds to L given by (1). In contrast, backward-propagating TE-mode light is converted into TM mode after traveling the same distance. Therefore, the optimal length of the device for nonreciprocal conversion is 0.27 mm. The performance index of the device is given by the NRPC

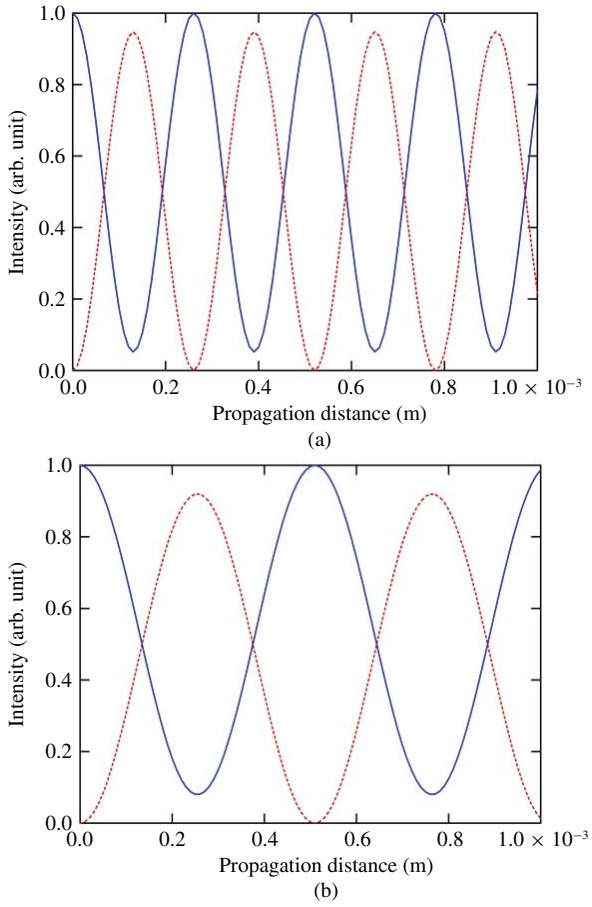

Fig. 5. Power distribution along the z-axis as a function of the propagation distance for TE-polarized input, for (a) forward and (b) backward propagation. (Solid curve) power distribution of TE component of light. (Dashed curve) power distribution of TM component.

efficiency, which is the conversion efficiency with which backward TE light is converted to TM in the device. An NRPC efficiency of 93% can be expected in our device.

III. Constructing the Device

To confirm our idea with actual devices, we made the trial device shown in Fig. 6. The device consists of an asymmetric InGaAsP waveguide grown on an InP substrate and a ferrimagnetic Ce:YIG layer bonded to the waveguide. Three NRPCs (three waveguides) on the substrate are shown in the figure. Square-shaped dummy InGaAsP regions (islands) were arrayed on both sides of each waveguide to support the YIG layer. The process for device formation was as follows.

A. Epitaxial Growth of InGaAsP on InP Substrate

The initial substrate was a non-doped 350-μm thick InP wafer with the crystal surface in the $< 100 >$ orientation. A non-doped InGaAsP layer of 1.1 μm thickness was grown on the substrate using metal-organic vapor-phase epitaxy in an RF-heated quartz reactor. The carrier gas was hydrogen (H_2). The source materials, mixed with the carrier gas, were trimethylindium [$(CH_3)_3In$], triethylgallium [$(C_2H_5)_3Ga$], tertiarybutylarsine (TBA), and tertiarybutylphosphine (TBP).

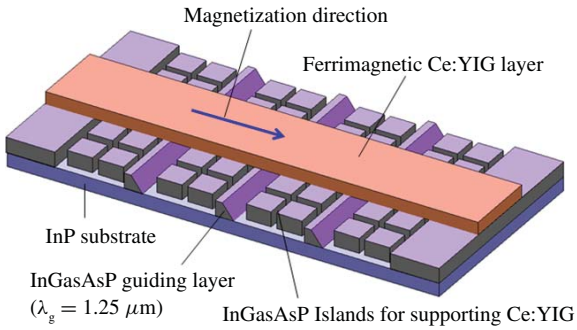

Fig. 6. Structure of NRPC device we made. Three NRPCs on InP substrate are shown. Square-shaped dummy InGaAsP regions (islands) were arrayed on both sides of each waveguide to support the YIG layer.

The growth temperature was 610 °C, and the growth rates was 20 nm/min. Under these conditions, the composition of the grown layer was $In_{0.75}Ga_{0.25}As_{0.54}P_{0.46}$ (absorption edge = 1.25 μm), which is lattice-matched to InP.

B. Forming Asymmetric Waveguides

The InGaAsP layer grown on the InP substrate was formed into asymmetric waveguides with a right-trapezoid cross section. Fig. 7 illustrates the forming process we used, showing the changing cross section of the waveguide. The process was as follows: A photoresist mask in the form of a waveguide pattern was made on the surface of the InGaAsP epitaxial layer [Fig. 7(a)]. The InGaAsP layer was etched chemically, using a mixture of Br_2, HBr, and H_2O [Fig. 7(b)]. This etching is anisotropic and attacks InGaAsP (and InP) preferentially in the (100) plane, thereby producing an asymmetric waveguide having a trapezoidal cross section with a base angle of 54°. By controlling a mixing rate of Br_2, HBr, and H_2O, we set the underetching rate of InGaAsP to 600 nm/min. We formed resist patterns with different widths of 2.0, 2.2, 2.4, 2.6, and 2.8 μm on the same substrate. After that, using underetching, we obtained waveguide patterns with reduced widths of 0.8, 1.0, 1.2, 1.4, and 1.6 μm. The photoresist mask was then removed [Fig. 7(c)]. A 200-nm SiO_2 layer was deposited on the wafer by means of oblique-angle electron-beam deposition. The left side of the waveguide was in the shadow of the waveguide and, therefore, not covered with SiO_2.

The exposed region of the waveguide (and the substrate) was vertically etched using reactive-ion etching with Cl_2 in an inductively coupled plasma reactor [Fig. 7(d)].

The SiO_2 layer was removed using buffered HF [Fig. 7(e)]. Fig. 8 shows the cross-sectional image observed with scanning electron microscopy.

This way, we made an asymmetric waveguide with an upper base w of 1 μm. We also made waveguides with $w = 1.2\ \mu$m and $w = 1.4\ \mu$m for comparison.

C. Wafer Bonding of Ce:YIG to InGaAsP Waveguides

A Ce:YIG layer was bonded directly to the InGaAsP waveguide [Fig. 6(f)] [16]. The Ce:YIG we used was a 500-nm thick epitaxial Ce:YIG grown on a (111) (Ca, Mg, Zr)-doped $Gd_3Ga_5O_{12}$ (SGGG) substrate with a thickness of 450 μm. To secure the adhesion between the bonded wafers, surface cleaning and activation of Ce:YIG and InGaAsP were necessary before bonding. As pretreatment, the surfaces of the Ce:YIG layer of the InGaAsP waveguide were slightly etched in dilute H_3PO_4 and HF, respectively. After that, two wafers were loaded into a vacuum chamber and exposed to an O_2 plasma for activating their surfaces. The Ce:YIG layer and the InGaAsP/InP wafer were brought into contact with a compression pressure of 1.5 MPa and heat-treated for 1 h at 250 °C in a vacuum chamber. This way, we bonded a 2.3-mm square YIG/GGG wafer to the InGaAsP/InP waveguide wafer with dimensions 2.3 mm by 3.4 mm.

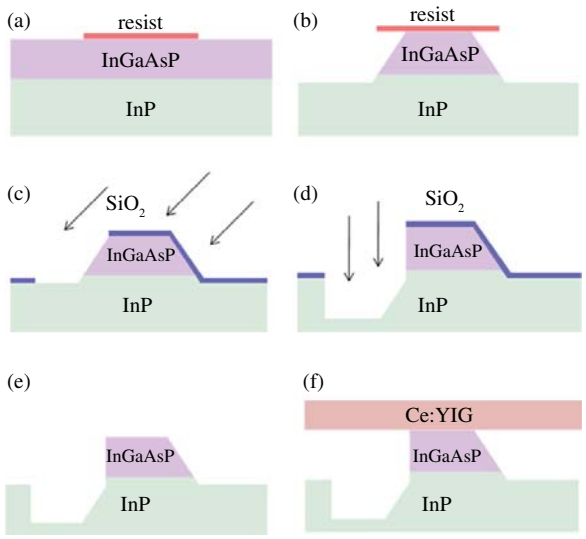

Fig. 7. (a)–(f) Forming process for asymmetric waveguides. In step (b), InGaAsP (111) plane (angle of 54°) was exposed with wet chemical etching using a mixture of Br_2, HBr, and H_2O.

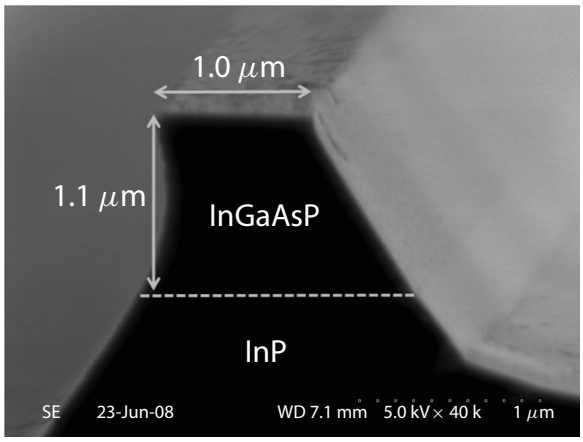

Fig. 8. Cross section of asymmetric waveguide observed with scanning electron microscopy.

D. Structure of Trial Devices

Fig. 9 shows the plane view of a trial device we made to confirm nonreciprocal polarization conversion; seven waveguides lying right and left on a device are shown. The total length is 3.4 mm and the length of the Ce:YIG/SGGG

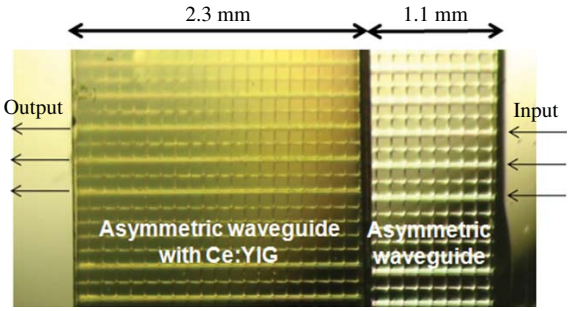

Fig. 9. Plane view of the device. Right side, by 1.1 mm in width, is not covered with Ce:YIG/GGG wafer.

is 2.3 mm. For the following optical measurements, we had to align an input optical fiber to one end of an individual waveguide of the device. To make this alignment easy, we left the right side of the device uncovered with the Ce:YIG because it was quite difficult through a thick Ce:YIG/SGGG wafer to measure the accurate vertical position of the waveguide. Fig. 10(a) and (b) shows enlarged oblique views of regions that are uncovered with the Ce:YIG/SGGG wafer.

For practical use, we have to make a 0.27-mm long waveguide (see Sec. II) covered wholly with a Ce:YIG layer and connect an optical fiber to the waveguide. For the present, however, we cannot yet manipulate such small devices for bonding, nor can we align fibers to wholly Ce:YIG-covered waveguides. Therefore, we used the trial device shown in Fig. 9 for measurements. From the measured data, we estimated the performance of the 0.27-mm long wholly Ce:YIG-covered device. The results are described in the next section.

IV. Device Operation

We confirmed that our device functioned successfully as an NRPC at 1.55 μm wavelength. Fig. 11 shows our experimental setup for measurement. As a light source, we made use of the amplified spontaneous emission (ASE) produced by an erbium-doped fiber amplifier. The ASE light was converted into TE-polarized light with a polarization controller and led to the device under test with an optical fiber. The light traveled through the device and went out through the left end. The output light from the device was collected by a lens and then measured with a power monitor (PM). The output light included a TM component in addition to the TE component. To measure the power separately for each component, we placed a TE-mode polarizer and then a TM-mode one in front of the PM. From measured power data for TE and TM, we calculated TM-conversion efficiency, i.e., the efficiency with which incident TE light is converted into TM in the device.

To operate the device, a magnetic field was applied parallel to the surface of the device and perpendicular to the waveguide. During measurement, the magnetic field for the device was set to 0.1 T. To measure the operation for forward and reverse propagations of light, we changed the polarity of the magnetic field instead of changing the direction of light propagation itself. The device was kept at 20 °C during the measurement.

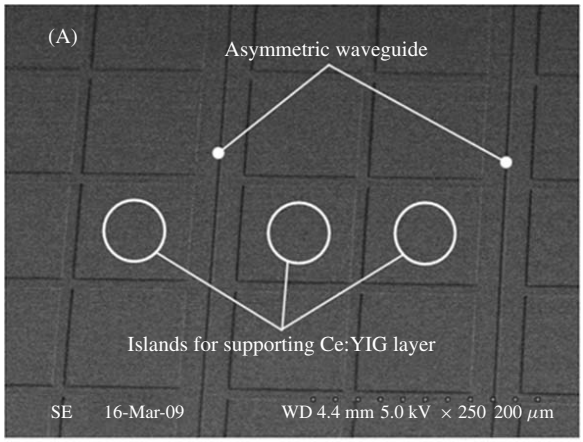

(a)

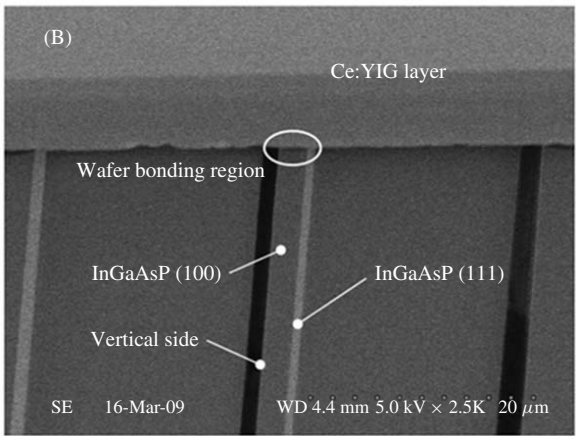

(b)

Fig. 10. Enlarged oblique views of trial device. (a) Waveguides and supporting islands. (b) Around the edge of Ce:YIG/SGGG wafer.

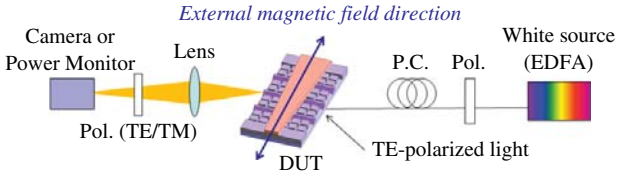

Fig. 11. Experimental setup to measure nonreciprocal polarization conversion in device.

Fig. 12 shows the transmission spectra of the device. The power of the output light from the device is plotted as a function of wavelength for TE-polarized and TM-polarized light. Fig. 12(a) is for forward propagation and (b) for backward propagation. The measured power varied with wavelength, this reflects the spectrum of the ASE light itself and is unrelated to the transmission characteristics of the device. Indeed, TM-conversion efficiency was almost independent of wavelength. The TM-conversion efficiency was different between forward and backward propagations, and this is positive proof for nonreciprocal rotation of the polarization plane of light traveling through the device. The intrinsic propagation loss in the device was about 6 dB, and the loss caused by the measurement system was estimated to be 22.5 dB. Fiber to the device coupling loss (about 7.5 dB) plus free-space coupling loss through the lens (about 15 dB).

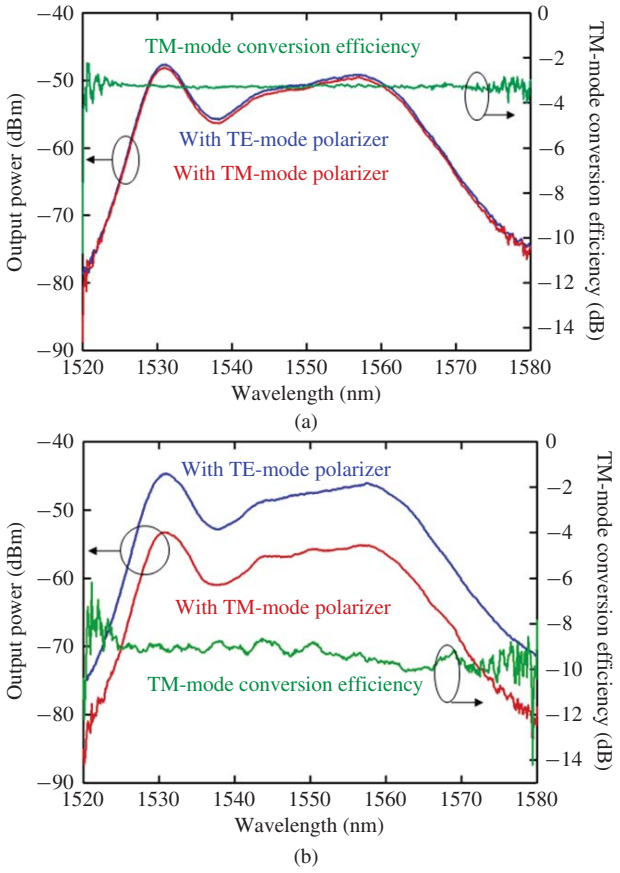

Fig. 12. Transmission power as a function of a wavelength from 1.52 to 1.58 μm for TE and TM light. (a) Forward and (b) backward propagation.

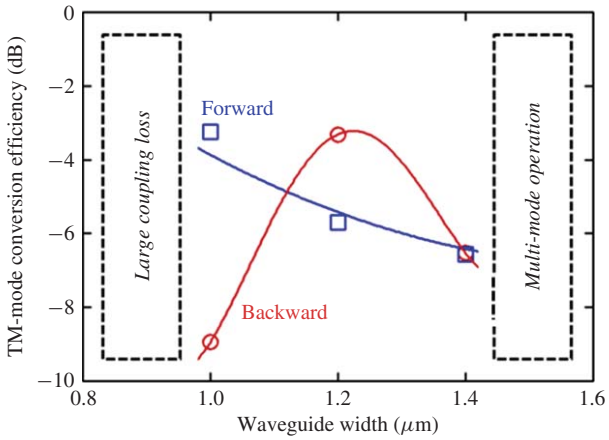

Fig. 13. TM conversion efficiency for forward and backward propagation as a function of waveguide width, at wavelengths of 1.52–1.58 μm.

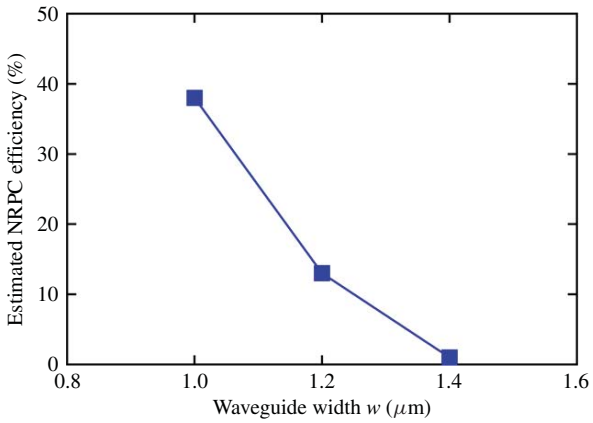

Fig. 14. Estimated NRPC efficiency of 0.27-mm long wholly YIG-covered device at 1.55 μm wavelength.

Fig. 13 plots TM-conversion efficiency as a function of waveguide width w for forward and backward propagation. Nonreciprocity was observed clearly for widths of 1 μm (the optimal width) and 1.2 μm.

As explained in Section III, our trial device had a part that was not covered with Ce:YIG (see Fig. 9), and this naked part produced *reciprocal* rotation of polarization. In addition, the trial device was longer than the optimum (= 0.27 mm), and this caused excessive rotation of polarization. The measured data shown in Figs. 12 and 13 include these unnecessary effects. We therefore quantified these effects with calculation using the Jones matrix method and deducted them from the measured data to estimate the NRPC efficiency (TM-conversion efficiency for backward propagation) for the 0.27-mm long wholly YIG-covered device. The result is shown in Fig. 14 as a function of waveguide width w. With our present technology, an NRPC efficiency of 38% can be obtained for $w = 1$ μm. NRPC efficiency decreases as waveguide width w increases. This is so because light is mainly distributed in the central part of the waveguide, and therefore an increase in cross-sectional size of the waveguide decreases the asymmetry that light experiences during its propagation.

V. Discussion and Conclusion

In this paper, we demonstrated an NRPC compatible with InP-based PICs for avoiding problems caused by undesired reflections of light. Using the experimental data, we estimated that the NRPC made with our present technology has an efficiency of 38%.

This efficiency is lower than the value (= 93%) we expected theoretically in Section II. One of the possible factors behind this is bonding nonuniformity across the device. It is not easy to achieve good adhesion between Ce:YIG and InGaAsP wafers over a large area. There is a possibility that bonding was imperfect in part of our trial device. One effective method of achieving better bonding is Ar-beam surface-activated bonding (SAB) [17]. We are now applying SAB to the wafer bonding of Ce:YIG and GaInAsP.

A more probable and important factor is that the shape of the waveguide in our trial device was not a perfect rib. For high NRPC efficiency, the InGaAsP asymmetric waveguide has to lie on a flat InP substrate as shown in Fig. 2. In practice, however, the substrate is not flat and the waveguide has a *raised-floor* structure, as shown in Fig. 7, because of the overetching in the formation of the waveguide. This probably affects the excitation of the two orthogonal modes in asymmetric waveguides (see [18]), thereby greatly reducing the NRPC efficiency of the device. This can be prevented if we can find an etchant that attacks InGaAsP but barely attacks

InP. We are now refining our fabrication technique to make a complete device for practical use.

REFERENCES

[1] R. Nagarajan, C. H. Joyner, R. P. Schneider, Jr., J. S. Bostak, T. Butrie, A. G. Dentai, V. G. Dominic, P. W. Evans, M. Kato, M. Kauffman, D. J. H. Lambert, S. K. Mathis, A. Mathur, R. H. Miles, M. L. Mitchell, M. J. Missey, S. Murthy, A. C. Nilsson, F. H. Peters, S. C. Pennypacker, J. L. Pleumeekers, R. A. Salvatore, R. K. Schlenker, R. B. Taylor, H. S. Tsai, M. F. Van Leeuwen, J. Webjorn, M. Ziari, D. Perkins, J. Singh, S. G. Grubb, M. S. Reffle, D. G. Mehuys, F. A. Kish, and D. F. Welch, "Large-scale photonic integrated circuits," *IEEE J. Sel. Topics Quantum Electron.*, vol. 11, no. 1, pp. 50–65, Feb. 2005.

[2] S. C. Nicholes, M. L. Mašanović, B. Jevremović, E. Lively, L. A. Coldren, and D. J. Blumenthal, "World's first InP 8×8 monolithic tunable optical router (MOTOR) operating at 40 Gbps line rate per port," in *Proc. Opt. Fiber Commun. Conf.*, 2009, no. PDPB1, pp. 1–3.

[3] H. Yokoi, T. Mizumoto, N. Shinjo, N. Futakuchi, and Y. Nakano, "Demonstration of an optical isolator with a semiconductor guiding layer that was obtained by use of a nonreciprocal phase shift," *Appl. Opt.*, vol. 39, no. 33, pp. 6158–6164, 2000.

[4] Y. Shoji, T. Mizumoto, H. Yokoi, I.-W. Osgood, and M. Richard, "Magneto-optical isolator with silicon waveguides fabricated by direct bonding," *Appl. Phys. Lett.*, vol. 92, no. 7, pp. 071117-1–071117-3, Feb. 2008.

[5] W. V. Parys, B. Moeyersoon, D. V. Thourhout, R. Baets, M. Vanwolleghem, B. Dagens, J. Decobert, O. L. Gouezigou, D. Make, R. Vanheertum, and L. Lagae, "Transverse magnetic mode nonreciprocal propagation in an amplifying AlGaInAs/InP optical waveguide isolator," *Appl. Phys. Lett.*, vol. 88, no. 7, pp. 071115-1–071115-3, Feb. 2006.

[6] T. Amemiya, H. Shimizu, Y. Nakano, P. N. Hai, M. Yokoyama, and M. Tanaka, "Semiconductor waveguide optical isolator based on nonreciprocal loss induced by ferromagnetic MnAs," *Appl. Phys. Lett.*, vol. 89, no. 2, pp. 021104-1–021104-3, Jul. 2006.

[7] H. Shimizu and Y. Nakano, "Fabrication and characterization of an InGaAsp/InP active waveguide optical isolator with 14.7 dB/mm TE mode nonreciprocal attenuation," *IEEE J. Lightw. Technol.*, vol. 24, no. 1, pp. 38–43, Jan. 2006.

[8] T. Amemiya, T. Tanemura, and Y. Nakano, "Nonreciprocal polarization converter consisting of asymmetric waveguide with magnetooptic cladding: Theory and simulation," *IEEE J. Quantum Electron.*, vol. 45, no. 7, pp. 769–776, Jul. 2009.

[9] L. M. Augustin, R. Hanfoug, J. J. G. M. van der Tol, W. J. M. de Laat, and M. K. Smit, "A compact integrated polarization splitter/converter in InGaAsP-InP," *IEEE Photon. Technol. Lett.*, vol. 19, no. 17, pp. 1286–1288, Sep. 2007.

[10] L. M. Augustin, J. J. G. M. van der Tol, R. Hanfoug, W. J. M. de Laat, M. J. E. van de Moosdijk, P. W. L. van Dijk, Y. S. Oei, and M. K. Smit, "A single etch-step fabrication-tolerant polarization splitter," *IEEE J. Lightw. Technol.*, vol. 25, no. 3, pp. 740–746, Mar. 2007.

[11] K. Saitoh and M. Koshiba, "Full-vectorial finite element beam propagation method with perfectly matched layers for anisotropic optical waveguides," *J. Lightw. Technol.*, vol. 19, no. 3, pp. 405–413, Mar. 2001.

[12] H. El-Refaei, D. Yevick, and T. Jones, "Slanted-rib waveguide InGaAsP-InP polarization converters," *IEEE J. Lightw. Technol.*, vol. 22, no. 5, pp. 1352–1357, May 2004.

[13] L. M. Augustin, J. J. G. M. van der Tol, E. J. Geluk, and M. K. Smit, "Short polarization converter optimized for active-passive integration in InGaAsP-InP," *IEEE Photon. Technol. Lett.*, vol. 19, no. 20, pp. 1673–1675, Oct. 2007.

[14] M. Fontaine, "Theoretical approach to investigating cross-phase modulation phenomena in waveguides with arbitrary cross sections," *J. Opt. Soc. Am. B*, vol. 14, no. 6, pp. 1444–1452, 1997.

[15] M. Fontaine, "Cross-phase modulation phenomena in strongly guiding waveguides: A theoretical approach revised," *J. Opt. Soc. Am. B*, vol. 15, no. 3, pp. 964–971, 1998.

[16] T. Mizumoto and H. Yokoi, "Waveguide optical isolators fabricated by wafer bonding," in *Proc. Mater. Res. Soc. Symp.*, vol. 834. 2005, pp. 135–146.

[17] H. Takagi, R. Maeda, and T. Suga, "Room-temperature wafer bonding of Si to $LiNbO_3$, $LiTaO_3$, and $Gd_3Ga_5O_{12}$ by Ar beam surface activation," *J. Micromech. Microeng.*, vol. 11, no. 4, p. 348, 2001.

[18] H. Deng, D. O. Yevick, C. Brooks, and P. E. Jessop, "Design rules for slanted-angle polarization rotators," *IEEE J. Lightw. Technol.*, vol. 23, no. 1, pp. 432–445, Jan. 2005.

Tomohiro Amemiya (S'06–M'09) received the B.Sc., M.Sc., and Ph.D. degrees in electronic engineering from the University of Tokyo, Tokyo, Japan, in 2004, 2006, and 2009, respectively.

He is currently with the Quantum Nanoelectronics Research Center, Tokyo Institute of Technology, Tokyo. His current research interests include physics of semiconductor light-controlling devices, optical spin-related devices, and the processing technology to fabricate these devices.

Dr. Amemiya is a member of the Optical Society of America and the Japan Society of Applied Physics. He was the recipient of the 2007 IEEE Photonics Society Annual Student Paper Award and the 2008 IEEE Photonics Society Graduate Student Fellowship.

Kenji Abe received the B.Sc. and M.Sc. degrees in electrical engineering from the Tokyo Institute of Technology, Tokyo, Japan, in 2007 and 2009, respectively.

He is currently with the Department of Electrical and Electronic Engineering, Tokyo Institute of Technology. His current research interests include waveguide optical devices and wafer bonding of dissimilar crystals, mainly focusing on the application to photonic integrated circuits.

Takuo Tanemura (S'02–M'06) received the B.E., M.S., and Ph.D. degrees in electronic engineering from the University of Tokyo, Tokyo, Japan, in 2001, 2003, and 2006, respectively.

He joined the Department of Electronic Engineering, University of Tokyo, in 2006, where he is currently with the Research Center for Advanced Science and Technology. He has been a Visiting Scholar at the Ginzton Laboratory, Stanford University, Stanford, CA, since 2010. He has authored or co-authored over 30 papers published in refereed journals and presented over 70 papers in international conferences. His current research interests include semiconductor photonic integrated circuits, photonic switching networks, and all-optical signal processing devices.

Dr. Tanemura is a member of the IEEE Photonics Society and the Institute of Information and Communication Engineers of Japan. He is the recipient of the 2005 IEEE LEOS Graduate Student Award and the 2006 Ericsson Young Scientist Award.

Tetsuya Mizumoto (S'81–M'84) received the B.E., M.E., and D.Eng. degrees in electrical engineering from the Tokyo Institute of Technology, Tokyo, Japan, in 1979, 1981, and 1984, respectively.

He is currently with the Department of Electrical and Electronic Engineering, Tokyo Institute of Technology, where he is also a Professor at the Graduate School of Science and Engineering. He has also been a Research Associate at the Tokyo Institute of Technology since 1984. His current research interests include waveguide optical devices, especially magnetooptic devices and all-optical switching devices based on third-order nonlinearity.

Dr. Mizumoto received the Treatise Award in 1994 and the Best Letter Award of the Electronics Society Transactions in 2007 from the Institute of Electronics, Information and Communication Engineers (IEICE). He is a fellow of IEICE, and a member of the Japan Society of Applied Physics and the Magnetic Society of Japan. He was awarded the IEEE Photonics Society Distinguished Lecturer award in July 2009.

Yoshiaki Nakano (S'81–M'87) received the B.E., M.S., and Ph.D. degrees in electronic engineering from the University of Tokyo, Tokyo, Japan, in 1982, 1984, and 1987, respectively. In 1984, he spent a year at the University of California, Berkeley, as an exchange student.

He joined the Department of Electronic Engineering, University of Tokyo, in 1987, and became an Associate Professor in 1992, a Professor in 2000, and the Department Head in 2001. He moved to the Research Center for Advanced Science and Technology, University of Tokyo, in 2002, where he is currently a Professor in the Department of Information Systems and the Director of the Center. In 1992, he was a Visiting Associate Professor at the University of California, Santa Barbara. He has authored or co-authored over 200 papers published in refereed journals, has presented over 400 papers in international conferences, and holds 40 patents. His current research interests include physics and fabrication technologies of semiconductor distributed feedback lasers, semiconductor optical modulators/switches, and monolithically integrated photonic circuits.

Dr. Nakano was an elected member of the Board of Governors of IEEE LEOS, a member of the Board of Directors of the Japan Society of Applied Physics (JSAP), and the Editor-in-Chief of *Applied Physics Express and Japanese Journal of Applied Physics*. He is currently a member of the Board of Directors of the Japan Institute of Electronics Packaging, the Chairman of the Optoelectronics Technology Trend Research Committee of the Optoelectronics Industry and Technology Development Association (OITDA), and the Chairman of the Optical Interconnect Standardization Committee of the Japan Electronics Packaging and Circuits Association. He is also a Fellow of the Institute of Electronics, Information, and Communication Engineers (IEICE) and of the JSAP, and a member of the IEEE EDS and the Optical Society of America. He is the recipient of the 1987 Shinohara Memorial Prize from the IEICE, the 1991 Optics Paper Award from the JSAP, the 1997 Marubun Science Prize, the 2007 Ichimura Prize, the 2007 IEICE Electronics Society Award, and the 2007 Sakurai Medal from the OITDA. He was presented the Prime Minister's Award in Collaborative Research between Academia and Industry in 2007. He served as the Project Leader of the Japanese National Project on "Photonic Networking Technology," organized by the Ministry of Economy, Trading, and Industry, and as the Project Leader of the SORST Program on "Nonreciprocal Semiconductor Digital Photonic Integrated Circuits and their Applications to Photonic Networking," sponsored by the Japan Science and Technology Corporation, Saitama, Japan.